Acta Crystallographica Section D
Biological Crystallography
ISSN 0907-4449

Mapping the active site of *Escherichia coli* malonyl-CoA–acyl carrier protein transacylase (FabD) by protein crystallography

Christian Oefner,[a]*‡ Henk Schulz,[a]‡ Allan D'Arcy[b] and Glenn E. Dale[a]‡

[a]Morphochem AG, Basel, Switzerland, and [b]Novartis Pharma AG, Werk Klybeck, Klybeckstrasse 141, WKL-127.P.74, CH-4057 Basel, Switzerland

‡ Present address: Arpida Ltd, Dammstrasse 36, CH-4142 Muenchenstein, Switzerland.

Correspondence e-mail: coefner@arpida.ch

Received 17 February 2006
Accepted 14 March 2006

PDB References: FabD complexed with glycerol, 2g1h, r2g1hsf; complexed with sulfate, 2g2o; complexed with malonate, 2g2y; complexed with malonyl-CoA, 2g2z.

Malonyl-CoA–acyl carrier protein transacylase (FabD; EC 2.3.1.39) is a key enzyme in the fatty-acid biosynthesis pathway of bacteria, catalyzing the transfer of a malonyl moiety from malonyl-CoA to holo acyl carrier protein (ACP), generating malonyl-ACP and free CoASH. Malonyl-ACP, which is the product of this reaction, is the key building block for *de novo* fatty-acid biosynthesis. Various binary complex structures of the *Escherichia coli* enzyme are presented, including that of the natural substrate malonyl-CoA, indicating the functional role of the highly conserved amino acids Gln11, Ser92, Arg117 and His201 and the stabilizing function of the preformed oxyanion hole during the enzymatic reaction. Based on the presented structural data, a possible new catalytic enzyme mechanism is discussed. The data obtained could be used in aiding the process of rational inhibitor design.

1. Introduction

Endogenous fatty acids are synthesized in all organisms in a pathway catalyzed by the fatty-acid synthase (FAS) complexes. In the type I system of mammals, including humans, FAS is a single large polypeptide composed of several distinct domains (Smith, 1994). In the type II system of bacteria, plants and protozoa, the FAS components, including the acyl carrier protein (ACP), exist as discrete proteins (Tsay *et al.*, 1992; Clough *et al.*, 1992; Waller *et al.*, 1998). The source of malonyl groups for normal fatty-acid and polyketide biosynthesis is malonyl-CoA. These three-carbon building blocks have to be transferred to the phosphopantetheine prosthetic groups of acyl carrier proteins (ACP) before they are further used in chain elongation by 3-oxoacyl-(acyl carrier protein) synthases (more commonly named β-ketoacyl ACP synthases).

Malonyl-CoA–acyl carrier protein transacylase (MCAT, FabD; EC 2.3.1.39) is a key enzyme in the fatty-acid biosynthesis pathway of bacteria. This enzyme catalyzes the transfer of a malonyl moiety from malonyl-CoA to holo ACP, generating malonyl-ACP and free CoA-SH (Magnuson *et al.*, 1993). Kinetic studies using a radioactive assay indicated an ordered ping-pong type of mechanism for the *Escherichia coli* enzyme and it has been shown that the transacylase is transiently malonylated at the active-site Ser92 (Joshi & Wakil, 1971; Ruch & Vagelos, 1973; Dreier *et al.*, 2001). The catalytic serine residue attacks the labile thioester bond of the

Table 1
Data-collection and refinement statistics.

Values in parentheses are for the outer shell.

	Sulfate complex	Glycerol complex	Malonate complex	Malonyl-CoA complex
Unit-cell parameters (Å)	$a = b = 83.11$, $c = 164.23$	$a = b = 83.15$, $c = 164.51$	$a = b = 83.30$, $c = 164.24$	$a = b = 83.34$, $c = 164.36$
Resolution range (Å)	20.0–1.76 (1.87–1.76)	20.0–1.86 (1.98–1.86)	20.0–2.26 (2.4–2.26)	20.0–2.80 (2.97–2.80)
No. of observed reflections	532227	252263	403220	99985
No. of unique reflections	57822	48061	27888	14482
R_{sym}† (%)	6.1 (50.7)	7.5 (54.6)	9.4 (52.4)	10.5 (55.9)
$I/\sigma(I)$	44.7 (4.7	18.1 (2.1)	27.4 (3.5)	17.5 (3.9)
Completeness (%)	100 (100)	97.5 (99.2)	100 (100)	96.9 (99.7)
Refinement statistics				
Resolution range (Å)	20.0–1.76	20.0–1.86	20.0–2.26	20.0–2.8
R_{cryst}‡ (%)	21.5	21.1	21.3	23.8
R_{free}‡ (%)	23.7	22.2	23.4	28.4
No. of protein atoms	2257	2257	2240	2257
No. of water molecules	223	178	103	11
No. of ligand atoms	5	6	7	54
Mean B for protein atoms (Å^2)	25.2	28.9	31.4	42.1
Mean B for ligand atoms (Å^2)	29.2	33.4	36.8	60.2
R.m.s.d.§ bonds (Å^2)	0.005	0.005	0.007	0.014
R.m.s.d. angles (°)	0.754	0.761	0.852	1.53

† $R_{sym} = \sum_h \sum_i |I_i(h) - \langle I(h)\rangle| / \sum_h \sum_i (h)$, where $I_i(h)$ and $\langle I(h)\rangle$ are the ith and mean measurement of the intensity of reflection h. ‡ $\sum_h ||F_{obs}| - |F_{calc}|| / \sum_h |F_{obs}|$, where $|F_{obs}|$ and $|F_{calc}|$ are the observed and calculated structure-factor amplitudes for the reflection h applied to the working (R_{cryst}) and test (R_{free}) sets, respectively. § R.m.s.d., root-mean-square deviation from the mean.

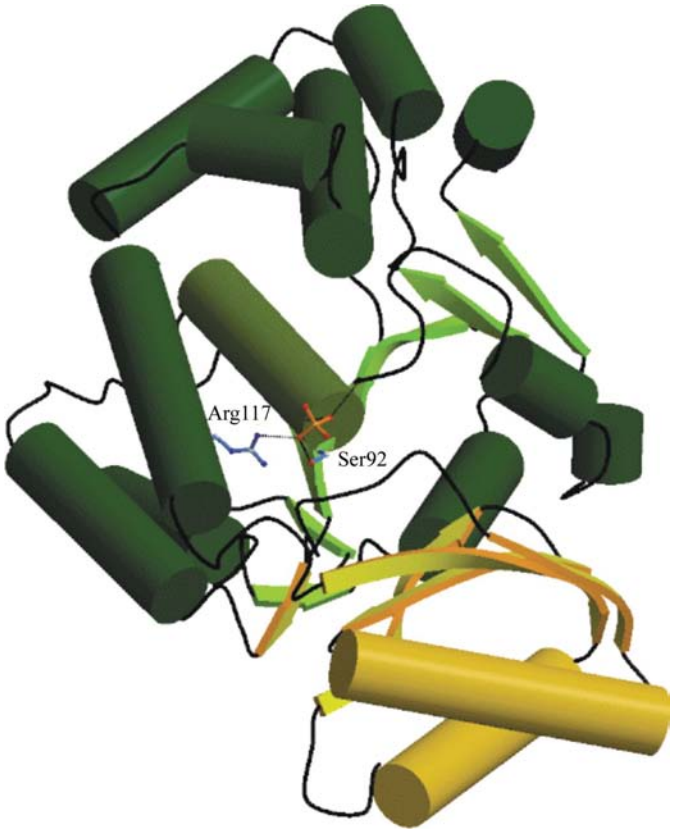

Figure 1
Schematic representation of the three-dimensional structure of *E. coli* FabD complexed with sulfate. The small molecule is shown in orange. Helices are indicated by cylinders and β-strands are shown as arrows. The small domain is highlighted in yellow. The active residues Arg117 and Ser92 are indicated and the active-site helix α6 is shown in light green.

incoming substrate, which leads to the formation of an acyl-enzyme complex and free CoASH. The malonyl moiety is subsequently transferred to the free thiol group of the phosphopantetheine arm of the acyl carrier protein (Joshi & Wakil, 1971). Malonyl-CoA–ACP transacylase does not transfer the acetyl group of acetyl-CoA, which is a weak competitive inhibitor, indicating the specificity of the enzyme for the malonyl moiety (Joshi & Wakil, 1971).

Genetic inactivation of the *fabD* gene has been shown to be lethal in all major pathogens investigated so far (Verwoert *et al.*, 1994; Zhang & Cronan, 1998). However, the enzyme has not been exploited as an antibacterial target and as yet no specific inhibitors have been discovered (Heath *et al.*, 2002; Campbell & Cronan, 2001). Recently, a continuous coupled enzyme assay for bacterial malonyl-CoA–Acp transacylase has been developed which, in combination with further structural information on the binding mode of small molecules, could facilitate the identification of FabD-specific inhibitors (Molnos *et al.*, 2003).

Structural data of the apo MCAT from *E. coli* obtained at 1.5 Å resolution reveal that the transacylase is best described as a distant relative of the α/β-hydrolase superfamily, possessing a hydrolase core with insertions of a helical flap and a ferredoxin-like subdomain (Serre *et al.*, 1995). Recently, the structure of malonyl-CoA–ACP transacylase from *Streptomyces coelicolor* has been solved in a complex with acetate at 2.0 Å resolution, revealing an invariant arginine bound to the small molecule that mimics the malonyl carboxylate (Keatinge-Clay *et al.*, 2003).

Here, we describe the crystal structures of binary complexes of a variety of small molecules bound to the active-site area of *E. coli* FabD and discuss the catalytic mechanism based on a binary enzyme–substrate complex. The structures reflect the

nature of the protein–ligand interactions and point towards the subsite specificity of the enzyme.

2. Materials and methods

E. coli FabD has been cloned, expressed, purified and crystallized as described previously (Molnos *et al.*, 2003; Serre *et al.*, 1994). Binary complexes were formed with the crystals obtained for the native enzyme in the presence of sulfate, glycerol, malonate and malonyl-CoA soaked at different concentrations in the molar range for several minutes. All crystals were flash-frozen in a cryoprotectant solution corresponding to the reservoir conditions with or without 30% glycerol and measured at 100 K as described in Table 1. In all cases the crystals are isomorphous with those of the native enzyme.

All crystals used for data collection belong to the tetragonal space group $P4_12_12$ with one molecule in the asymmetric unit. For data collection, diffraction intensities were obtained with Cu $K\alpha$ radiation provided by a Nonius FR591 rotating-anode generator equipped with an Osmic mirror system and recorded on a MAR Research image-plate area detector. All diffraction data were processed and scaled with *DENZO* and *SCALEPACK* (Otwinowski, 1993) and further analyzed with the *CCP*4 program suite (Collaborative Computational Project, Number 4, 1994). The initial phases were calculated for the native enzyme using the deposited structure of native malonyl-CoA–acyl carrier protein transacylase (PDB code 1mla; Serre *et al.*, 1995). Model bias has been minimized by omitting all water molecules from the initial model. Iterative rounds of model building were performed with *MOLOC* (Gerber, 1992) and stereochemically restrained positional and temperature-factor refinement was performed with *REFMAC* (Murshudov *et al.*, 1997) using parameters for ideal stereochemistry as described by Engh & Huber (1991). In each complex structure, a difference Fourier map revealed residual electron density located in the active-site area corresponding to the bound molecule. Progressive introduction of solvent molecules with good geometry led to the binary complexes, as summarized in Table 1.

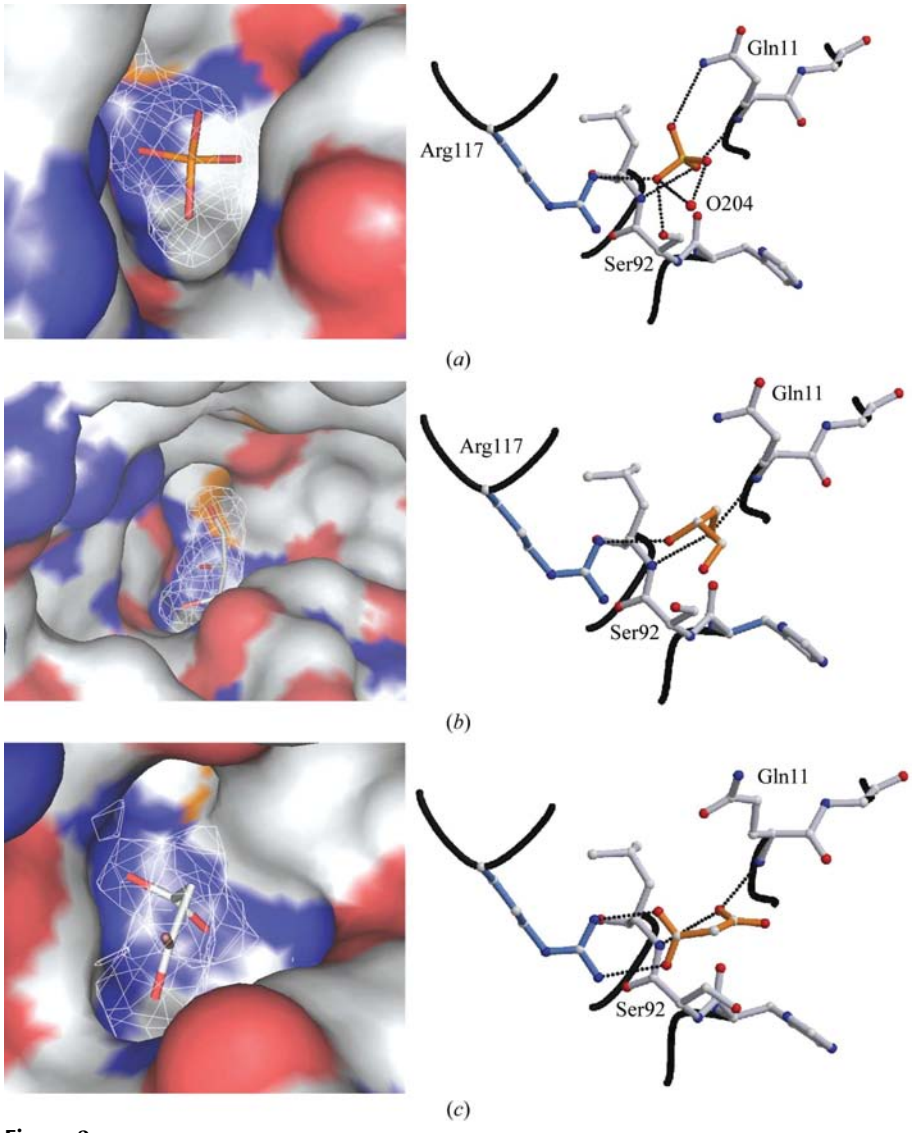

Figure 2
Small-molecule binding to the active site of *E. coli* FabD. (*a*) shows sulfate binding, (*b*) the binding of glycerol and (*c*) the intermolecular interaction with malonate. The left part of each figure shows the molecular surface of the active-site region together with the small molecule and the final $2F_o - F_c$ electron-density map. All maps are contoured at 1σ and are shown in white mesh. The molecular surfaces are coloured by electrostatic potential: red, negative; blue, positive. The figures were generated using *PyMOL* (DeLano, 2001). The right-hand figures show the electrophilic interactions of the small molecules with the enzyme. Hydrogen bonds are indicated by dotted lines and water molecules are shown as red spheres. These figures were generated with the programs *MOLSCRIPT* (Kraulis, 1991) and *RASTER3D* (Merritt & Bacon, 1997).

3. Results and discussion

The fold of the enzyme has been described (Serre *et al.*, 1995) as that of an α/β protein of 307 amino acids in length comprising two non-contiguous subdomains. The smaller domain, which contains a four-stranded antiparallel β-sheet capped by two α-helices, is embedded within the larger one and contains residues 124–205. The larger domain contains a short four-stranded parallel β-sheet and 12 α-helices of 4–17 residues in length (Serre *et al.*, 1995; Keatinge-Clay *et al.*, 2003) (Fig. 1). The active site of the enzyme is located in a gorge formed by the two subdomains in which the guanidinium group of Arg117 is rigidly positioned at its base. Arg117

belongs to a group of four invariant residues within the active-site region together with Ser92, His201 and Gln11 and is involved in the recognition of the free carboxyl group of the substrate *via* electrostatic interactions.

The structural data of the native enzyme, obtained at 1.76 Å resolution from crystals grown in 50% ammonium sulfate, clearly indicate that a single molecule of sulfate from the crystallization buffer is bound to MCAT and interacts with the guanidinium group of the conserved arginine residue (Fig. 2*a*). O3 of the sulfate ion is involved in three intermolecular hydrogen bonds. It interacts with of Arg117 NH1 at a distance of 2.83 Å and the hydroxyl group of Ser92 (2.6 Å) and is further involved in a hydrophilic interaction with water molecule 204 (2.73 Å). O5 of the ion is stabilized by the enzyme through a hydrogen bond formed with Gln11 NE2 (3.4 Å) and the small molecule shows an interaction of the oxygen O2 with the oxyanion hole, which is formed by the main-chain amides of Gln11 and Leu93. Finally, O4 of the anion is involved in a hydrophilic interaction with water 204, which completes the possible hydrogen-bond formation.

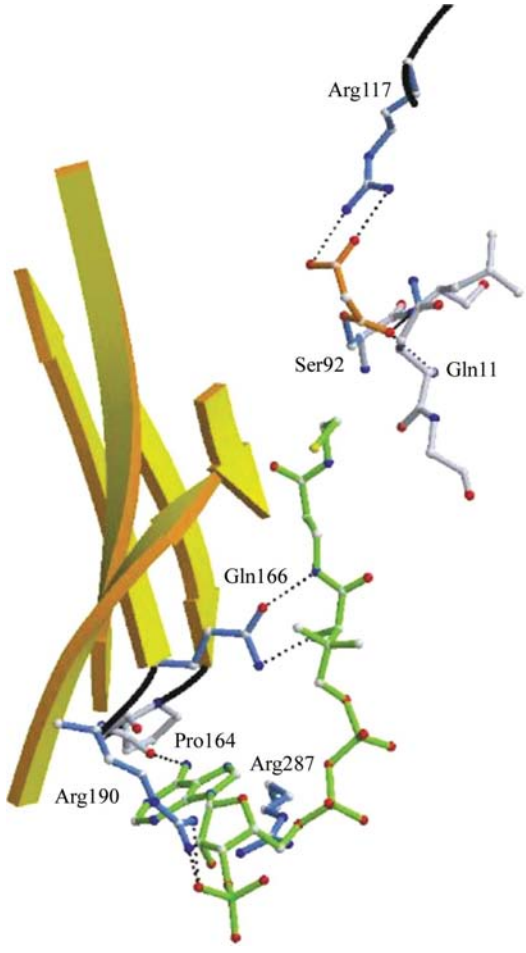

Figure 3
Malonyl-CoA binding to FabdD. The malonyl moiety of the processed substrate is covalently bound to the catalytic serine residue 92 *via* an oxo-ester bond. Hydrogen bonding is indicated by dotted lines. The figure was generated with the programs *MOLSCRIPT* (Kraulis, 1991) and *RASTER3D* (Merrit & Bacon, 1997).

The structural data of the native enzyme using crystals stabilized with glycerol as cryoprotectant clearly indicate that a single molecule of glycerol is bound in the active site. Similar to the sulfate complex, glycerol forms a single hydrogen bond with Arg117 NH1 *via* the O atom of its secondary carbon as determined at 1.86 Å resolution (Fig. 2*b*). The hydrogen-bonding distance is 2.81 Å, positioning the hydroxyl group at position 1 such that it interacts with the oxyanion hole of the enzyme *via* two hydrogen bonds with distances of 2.98 and 3.02 Å.

The 2.26 Å data obtained from crystals of the native enzyme soaked with malonate show similar electrostatic interactions with both amino groups of the oxyanion hole as those observed with glycerol. In addition, malonate forms a bidentate salt bridge with Arg117 NH1 and NH2, with bonding distances of 2.53 Å for O5 and 2.74 Å for O3, respectively, as determined at 2.26 Å resolution (Fig. 2*c*). The planes of both carboxylate moieties are oriented perpendicular to one another, with that involved in salt-bridge formation with Arg117 being coplanar with the guanidinium group of the conserved residue. Neither in the complex with glycerol nor in the complex with malonate is the catalytic serine residue involved in intermolecular hydrogen-bond formation. The side-chain orientation, however, is altered within the structures by varying the χ_1 angle from −166 to −39°.

All three small molecules directly interact with the enzyme *via* electrostatic interactions involving the key structural features needed for substrate recognition. This includes the pronounced interaction with the oxyanion hole formed by the main-chain amides of Gln11 and Leu93. Except for the binary complex with malonate, the hydroxyl group of the catalytic serine side chain is within hydrogen-bonding distance of NE2 of the conserved histidine residue 201. This preformed side-chain conformation is altered upon malonate binding, most likely to avoid sterical conflicts with the bound small molecule.

The soaking experiment of the substrate malonyl-CoA in the presence of 60% phosphate pH 6.0 for approximately 5 min clearly revealed the cleavage of the substrate and the binding of the malonyl and coenzyme A moieties to the enzyme as determined at 2.8 Å resolution (Fig. 3). The binding interactions of the processed substrate with the enzyme indicate that the malonyl transfer, which is catalyzed by FabD in the presence of holo-ACP, involves the entire length of the gorge. The labile thioester bond of the incoming substrate has been attacked by the active-site serine residue 92 and the malonyl moiety of the processed substrate remains covalently bound to the catalytic residue *via* an oxo-ester bond. The complex is stabilized by the oxyanion hole of the enzyme, which is formed by the main-chain amides of Gln11 and Leu93. In addition, the carboxylate of malonyl interacts with the guanidinium moiety of Arg117 *via* a bidentate salt bridge, as observed for malonate binding, and its central axis is parallel to the ester bond formed with the catalytic residue, which is clearly defined in the electron density.

The CoA-SH moiety of the processed substrate is located along the gorge above the four-stranded antiparallel β-sheet of the small domain. It involves a number of hydrogen bonds,

which are formed with the side chain of Gln166 and the central pantothenic acid moiety of the product. The side chain of the glutamine residue alters its conformation compared with that observed for the small-molecule complexes. The central hydrophobic dimethyl moiety of the product as well as the hydrophobic face of the remaining panthothenic acid moiety are nearly coplanar with the β-sheet backbone of the small domain. This part of the protein involves the side chains of Met132, Ala134, Ile136, Val159, Val168, Leu192, Leu194 and Val196. Furthermore, it is only the terminal base and phosphate moiety of the product which are clearly defined in the electron density. Their binding is mediated through hydrogen bonding with the side chain of Ser163 and the main-chain carbonyl of Pro164. In addition, hydrophobic interactions are observed with Ile136 and the hydrophobic face of the guanidinium group of Arg287. There is no clear intermolecular interaction present of either bridging phosphate moiety with the enzyme.

The structural data obtained for the FabD–malonyl-CoA complex clearly indicate the catalytic role of Ser92 and supports the reaction mechanism proposed by Keatinge-Clay *et al.* (2003) (Fig. 4). After malonyl-CoA is bound, Ser92 attacks the thioester carbonyl, forming a tetrahedral intermediate stabilized through a favourable interaction with the oxyanion hole. As proposed, the thioester carbonyl inserts into the oxyanion hole, with the thioester plane being nearly perpendicular to that of the terminal carboxylate. During the enzyme reaction, the thioester carbonyl group is positioned at the N-terminal region of the conserved active-site helix α6 of the larger domain, thereby placing the reaction centre under the influence of a positive helical dipole moment (Hol, 1985). Therefore, it seems to be the environment of the active site which destabilizes the labile thioester bond of the substrate upon binding, similarly to the situation observed for 4-hydroxybenzoyl-CoA thioesterase and β-ketoacyl synthases (Thoden *et al.*, 2002; Price *et al.*, 2001). The carbonyl group is positioned in the oxyanion hole and stabilized *via* hydrogen bonds, which further enhances the polarization of the electron density away from the carbonyl carbon and makes the scissile bond more susceptible to nucleophilic attack. The imidazole side chain of His201 positions the hydroxyl function of the serine residue for substrate attack, leading to the formation of a tetrahedral intermediate in which the thioester carbonyl inserts into the oxyanion hole with the thioester plane being nearly perpendicular to that of the terminal carboxylate (Keatinge-Clay *et al.*, 2003). The side chain of His201 subsequently forms a hydrogen bond with the terminal malonyl group as observed for the cleaved substrate. This is also consistent with the observation that a His211Ala mutant in malonyl-CoA–ACP transacylase from *S. coelicolor* has no detectable catalytic activity (Dreier *et al.*, 2001). The presence of an unambiguously defined malonyl moiety covalently linked to the catalytic serine residue supports the observation that the acyl-enzyme complex is stable in aqueous solution (Donadio *et al.*, 1991). The position of the newly formed ester bond with respect to the oxyanion then allows the malonyl transfer to the free thiol group of the phosphopantotheine arm of the acyl carrier protein (Joshi & Wakil, 1971).

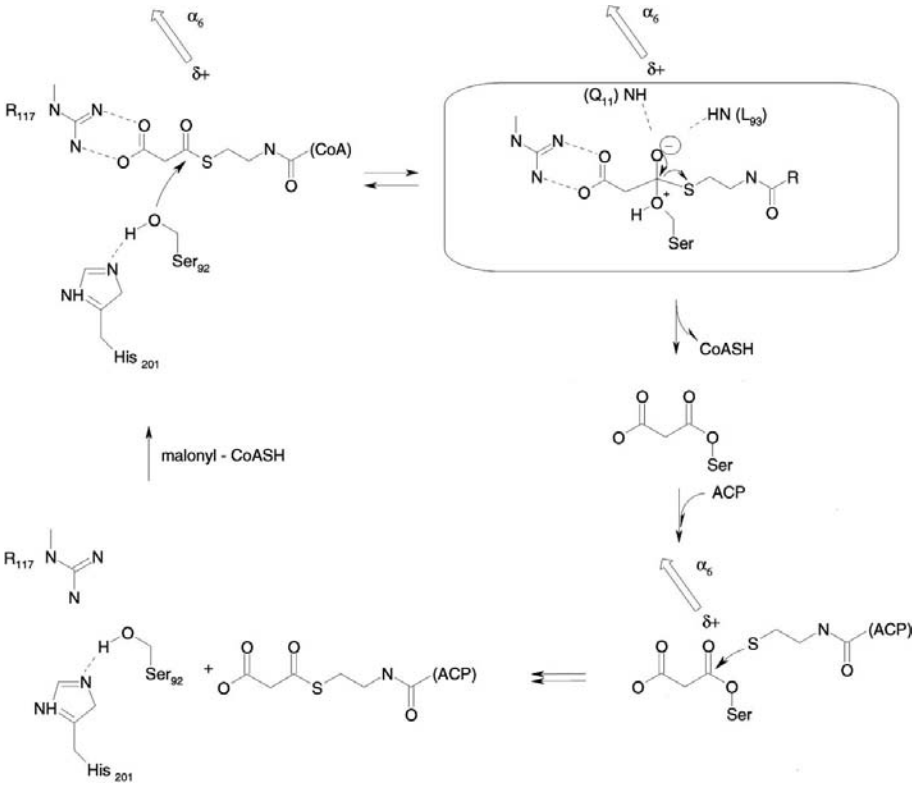

Figure 4
Reaction mechanism.

It is the conserved basic arginine residue 117 located at the bottom of the gorge which is involved in the recognition of the acidic part of the substrate. Its role and function is also confirmed by the binding of various small molecules *e.g.* sulfate, glycerol and malonate. They mimic the carboxyl end of the covalently bound malonyl group as does acetate in the structure of malonyl-CoA–ACP transacylase from *S. coelicolor* (Keatinge-Clay *et al.*, 2003). However, it is only malonate which is involved in a bidentate salt bridge with Arg117, an interaction also observed for bound substrate. Common to all binary complexes of the *E. coli* enzyme is the involvement of the oxyanion hole in small-molecule binding, which further stabilizes the intermolecular interactions of the enzyme. For malonate binding, the observed perpendicular arrangement of both bound carboxylate groups is in agreement with that proposed for substrate recognition (Keatinge-Clay *et al.*, 2003). The authors proposed that the thioester carbonyl inserts into the oxyanion hole, with the

thioester plane being nearly perpendicular to that of the terminal carboxylate.

4. Conclusion

The present study defines in detail the intermolecular interactions required for small-molecule recognition and substrate catalysis and raises the question of the drugability of the enzyme. It is the length of the substrate as well as its amphiphatic character that define the subsite specificity of the enzyme. To use FabD as an antibacterial target, the question of which parts have be taken into account remains to be answered.

We gratefully acknowledge the excellent technical assistance of Dr Aengus MacSweeney and thank Dr S. Pierau for careful reading of the manuscript.

References

Campbell, J. W. & Cronan, J. E. Jr (2001). *Annu. Rev. Microbiol.* **55**, 305–332.
Clough, R. C., Matthis, A. L., Barnum, S. R. & Jaworski, J. G. (1992). *J. Biol. Chem.* **267**, 20992–20998.
Collaborative Computational Project, Number 4 (1994). *Acta Cryst.* D**50**, 760–763.
DeLano, W. L. (2001). *The PyMOL User's Manual.* DeLano Scientific, San Carlos, CA, USA.
Donadio, S., Staver, M. J., McAlpine, J. B., Swanson, S. J. & Katz, L. (1991). *Science*, **252**, 675–679.
Dreier, J., Li, Q. & Koshland, C. (2001). *Biochemistry*, **40**, 12407–12411.
Engh, R. & Huber, R. A. (1991). *Acta Cryst.* A**47**, 392–400.
Gerber, P. (1992). *Biopolymers*, **32**, 1003–1017.
Heath, R. J., White, S. W. & Rock, C. O. (2002). *Appl. Microbiol. Biotechnol.* **58**, 695–703.
Hol, W. (1985). *Adv. Biophys.* **19**, 1333–165.
Joshi, V. C. & Wakil, S. J. (1971). *Arch. Biochem. Biophys.* **143**, 493–505.
Keatinge-Clay, A. T., Shelat, A. A., Savage, D. F., Tsai, S. C., Miercke, L. J., O'Connell, J. D. III, Khosla, C. & Stroud, R. M. (2003). *Structure*, **11**, 147–154.
Kraulis, P. J. (1991). *J. Appl. Cryst.* **24**, 946–950.
Magnuson, K., Jackowski, S., Rock, C. O. & Cronan, J. E. Jr (1993). *Microbiol. Rev.* **57**, 522–542.
Merritt, E. A. & Bacon, D. J. (1997). *Methods Enzymol.* **277**, 505–524.
Molnos, J., Gardiner, R., Dale, G. E. & Lange, R. (2003). *Anal Biochem.* **319**, 171–176.
Murshudov, G. N., Vagin, A. A. & Dodson, E. J. (1997). *Acta Cryst.* D**53**, 240–255.
Otwinowski, Z. (1993). *Proceedings of the CCP4 Study Weekend. Data Collection and Processing*, edited by L. Sawyer, N. Isaacs & S. Bailey, pp. 56–62. Warrington: Daresbury Laboratory.
Price, A. C., Choi, K. H., Heath, R. J., Li, Z., White, S. W. & Rock, C. O. (2001). *J. Biol. Chem.* **276**, 6551–6559.
Ruch, F. E. & Vagelos, P. R. (1973). *J. Biol. Chem.* **248**, 8086–8094.
Serre, L., Swenson, L., Green, R., Wei, Y., Verwoert, I. I., Verbree, E. C., Stuitje, A. R. & Derewenda, Z. S. (1994). *J. Mol. Biol.* **242**, 99–102.
Serre, L, Verbree, E. C., Dauter, Z., Stuitje, A. R. & Derewenda, Z. S. (1995). *J. Biol. Chem.* **270**, 12961–12964.
Smith, S. (1994). *FASEB J.* **15**, 1248–1259.
Thoden, J. B., Holden, H. M., Zhuang, Z. & Dunaway-Mariano, D. (2002). *J. Biol. Chem.* **277**, 27468–27476.
Tsay, J. T., Oh, W., Larson, T. J., Jackowski, S. & Rock, C. O. (1992). *J. Biol. Chem.* **267**, 6807–6814.
Verwoert, I. I., Verhagen, E. F., van der Linden, K. H., Verbree, E. C., Nijkamp, H. J. & Stuitje, A. R. (1994). *FEBS Lett.* **348**, 311–316.
Waller, R. F., Keeling, P. J., Donald, R. G., Striepen, B., Handman, E., Lang-Unnasch, N., Cowman, A. F., Besra, G. S., Roos, D. S. & McFadden, G. I. (1998). *Proc. Natl Acad. Sci. USA*, **95**, 12352–12357.
Zhang, Y. & Cronan, J. E. Jr (1998). *J. Bacteriol.* **180**, 3295–3303.